Energy 171 (2019) 135–148

Contents lists available at ScienceDirect

Energy

journal homepage: www.elsevier.com/locate/energy

CMIP-5 models project photovoltaics are a no-regrets investment in Europe irrespective of climate change

Johannes Müller [a, *], Doris Folini [a], Martin Wild [a], Stefan Pfenninger [b]

[a] Institute for Atmospheric and Climate Science, ETH Zurich, CH-8092 Zurich, Switzerland
[b] Institute for Environmental Decisions, ETH Zurich, CH-8092 Zurich, Switzerland

ARTICLE INFO

Article history:
Received 30 July 2018
Received in revised form
25 November 2018
Accepted 18 December 2018
Available online 27 December 2018

Keywords:
Climate change impact
Solar photovoltaic energy
Energy scenarios
Europe

ABSTRACT

Using projections of surface solar radiation and temperature from 23 CMIP5 global climate models for two climate change scenarios (RCP4.5 & 8.5) we quantify the average change in PV electricity production expected in the years 2060–2080 compared to the present (2007–2027). We upsample daily radiation data to hourly resolution with a sinusoidal diurnal cycle model and split it into direct and diffuse radiation with the semi-empirical BRL model as input to a PV electricity generation model. Locally, changes in PV potential from −6% to +3% in annual and −25% to +10% in monthly means are shown. These projections are combined with a PV deployment scenario and show countries benefitting from increased PV yields include Spain, France, Italy and Germany. We also calculate uncertainties when calculating PV yield with input data at daily or lower resolution, demonstrating that our method to derive synthetic hourly profiles should be of use for other researchers using input data with low temporal resolution. We conclude that PV is an attractive and no-regrets investment in Europe irrespective of future climate change, and can continue to play a key role in energy system decarbonisation.

1. Introduction

Over the last decade, solar power has become an essential technology in the realisation of a sustainable energy system in Europe. Installed electricity generation capacity of solar photovoltaic (PV) grew from 5 up to 101 GWp, with investments made primarily in Germany, Italy and the United Kingdom [13,14]. Driven ultimately by increasing concern about the potential effects of anthropogenic climate change, the proximate cause of this rapid deployment is a dramatic decline in the cost of PV systems [27,36]. However, even with large scale deployment of PV, other renewable energy technologies, and increased efforts in Greenhouse Gas (GHG) mitigation, the repercussions of decades of GHG emissions cannot be averted. In other words, the world is already committed to a certain degree of climate change.

Climate change will very likely cause temperatures in Europe to increase in the future [31]. Increasing temperatures will lead to changes in precipitation patterns and associated cloud fields. Together with changes in atmospheric aerosol composition, surface irradiance will also be affected. These two variables, irradiance and temperature, are directly responsible for the amount of electric power a solar PV panel can produce. Hence PV electricity generation will be indirectly influenced by climate change. The rise in temperature should lead to an almost linear decrease in efficiency of PV panels, due to an almost constant sensitivity of $-0.5\%\,^{\circ}C^{-1}$ [25]. The quantification of effects from changes in irradiance, however, are not straightforward. First, the response of PV electricity output to changes in irradiance is non-linear, especially at low intensities. Second, for tilted panels, due to geometric reasons, the effect of irradiance changes depends on the ratio between direct and diffuse radiation. Changes in cloud cover and atmospheric aerosol composition will affect this ratio as well. This dependency of PV power on environmental factors introduces a potentially large uncertainty for investment, so a better quantification of these effects may help to promote investments in future PV power plants. Additionally, the intra-annual distribution of energy yield is of great interest as it aids in the planning of storage solutions for the variable electricity generation of PV systems.

Here we aim to answer the question of how future changes in climate will affect the potential of PV power plants in Europe, what roles individual environmental variables (irradiance and temperature) play and how the future European energy system could be affected by these changes. A previous study by Wild et al. [35],

* Corresponding author.
E-mail addresses: muelljoh@student.ethz.ch, j.c.mueller@gmx.ch (J. Müller).

https://doi.org/10.1016/j.energy.2018.12.139
0360-5442/

List of symbols

Variables

β	Solar altitude [°]
ε	Plane incidence angle [°]
η_{rel}	Instantaneous efficiency of a panel relative to standard test conditions
ψ	Persistent index used in BRL model
a_P	Panel azimuth [°]
a_S	Solar azimuth angle [°]
AST	Apparent solar time
dt	Number of hours between sunrise and sunset
h	Hour at which instantaneous irradiance value I_h is calculated
I_h	Instantaneous irradiance value
$I_{dif,h}$	Diffuse horizontal irradiance [W m^{-2}]
$I_{dif,p}$	Diffuse irradiance on the panel [W m^{-2}]
$I_{dir,h}$	Direct horizontal irradiance [W m^{-2}]
$I_{dir,p}$	Direct irradiance on the panel [W m^{-2}]
$I_{tot,h}$	Total horizontal irradiance ($I_{dir,h} + I_{dif,h}$) [W m^{-2}]
$I_{tot,p}$	Total irradiance on the panel ($I_{dir,p} + I_{dif,p}$) [W m^{-2}]
k_d	Fraction of diffuse horizontal irradiance from the total horizontal irradiance $\left(\frac{I_{dif,h}}{I_{tot,h}}\right)$
K_t	Daily atmospheric clearness index
k_t	Hourly atmospheric clearness index
S_r	Sunrise hour
S_s	Sunset hour
t	Panel tilt [°]
T_{amb}	Ambient temperature [°C]

CMIP5 variables

rsds	Surface downwelling shortwave radiation or all-sky shortwave radiation [W m^{-2}]
rsdscs	Surface downwelling shortwave radiation assuming clear sky or clear-sky shortwave radiation [W m^{-2}]
tas	Near-surface air temperature [°C]

Constants

A	Surface albedo (= 0.3)
G_{STC}	Ambient temperature at standart test conditions(= 1000 W m^{-2})
T_{STC}	Ambient temperature at standart test conditions (= 25°)

based on the methodology by Crook et al. [7] set out with a similar goal, also focusing on future trends in PV electricity generation potential relying on annual and seasonal climate projection data from Climate Model Intercomparison Project Phase 5 (CMIP5). The present study is based on data from the CMIP5 as well. Up to 23 Global Climate Models (GCMs) for Representative Concentration Pathways (RCPs) 4.5 and 8.5 each were used. RCPs describe different possible future climates depending on anthropogenic emission scenarios. They are characterised by the magnitude of radiative forcing in W m^{-2} reached by 2100, which is represented by the number in their name. The spread of these models can be regarded as the uncertainty of the input data for the predictions in this study. We use the variables for surface downwelling all-sky shortwave radiation, which simulates realistic surface irradiances, including influences through cloud cover and atmospheric composition as well as the near-surface air temperature. The CMIP5 data is input in the PV electricity generation model Global Solar Energy Estimator (GSEE) which calculates the energy output of a solar panel on an hourly basis [29]. The present study uses CMIP5 data with daily resolution, compared to annual and seasonal mean values used in Ref. [35]. This allows us to examine changes in PV yields at a monthly mean resolution and to assess the stability and fluctuations in energy yield throughout the year. In addition, GSEE is a more advanced model for the calculation of the electric power output, which factors in direct and diffuse radiation as well as temperature. Jerez et al. [24] used the EURO-CORDEX regional climate model ensemble for a similar analysis, however the PV model used in that study lacks the inclusion of the diffuse radiation into the calculations as well. Based on an unpublished analysis with GSEE we found that for tilted panels it is highly relevant to distinguish between the direct and diffuse radiation. Also [24] uses five Regional Climate Models (RCMs) as a data source, while we calculate climate change impact based on 23 GCMs from the CMIP5. Additional local studies [4,28] found a slight increase in solar resources in the future in Greece and in the south of the UK. Pangea et al. [28] based their analysis on five RCMs while [4] used probabilistic climate change projections from the UKCP09 model. Gaetani et al. [17] examined data from ECHAM5-HAM climate model to estimate the near future change in productivity of PV energy in Europe and Africa.

The remainder of this paper proceeds as follows. After discussing the methods, including the setup of how CMIP5 data can be processed with GSEE, we present results showing the changes to potential energy yield from PV panels across Europe. In addition, we show sensitivity analyses based on the differing effect of temperature and irradiance, the role of cloudiness and atmospheric composition, temporal resolution of input data and the method used to upsample to hourly data. Finally, not every country will experience the same PV sector development. In order to illustrate which parts of Europe may be most affected by climate change induced PV productivity changes, we pair projections of PV electricity generation potential with a scenario of how the European energy system may evolve.

2. Data and methods

Our PV projections rely on a PV electricity generation model (Sect. 2.1) [29] that feeds on climate model data (Sect. 2.2) which has been appropriately pre-processed (Sect. 2.3) and adapted to scenarios of future development of PV installations (Sect. 2.4). The pre-processing bridges the gap between what data is typically available and what data is actually needed as input for the PV electricity generation model. Its performance is estimated based on comprehensive historical reanalysis data (Sect. 2.5).

2.1. GSEE PV electricity generation model

To simulate the electricity output at a given location we use the PV electricity generation model called Global Solar Energy Estimator (GSEE) [29]. It uses three environmental parameters: total horizontal irradiance ($I_{tot,h}$, sum of direct and diffuse radiation), fraction of diffuse irradiance from the total horizontal irradiance (k_d), and ambient temperature (T_{amb}), as well as several panel-specific parameters (coordinates, tilt and azimuth angles, peak generation capacity, panel tracking mode) as input variables to calculate the PV electricity output on an hourly basis. These three

environmental parameters must be available in hourly resolution. An assessment of the performance of GSEE can be found in Ref. [29].

GSEE computes the electric power output in two steps. First, the model calculates the direct $I_{dir,p}$ and diffuse $I_{dif,p}$ irradiance on the panel from the total horizontal irradiance ($I_{tot,h}$) and the diffuse fraction (Eqs. (1) and (2)), while taking the panel's orientation (panel tilt t, panel azimuth a_P) and the sun's position (solar altitude β, solar azimuth angle a_S) into account [29], with ε being the panel incidence angle (Eq. (3)) and A the surface albedo ($= 0.3$).

$$I_{tot,p} = I_{dir,p} + I_{dif,p}, \qquad I_{dir,p} = \frac{I_{dir,h} \times \cos(\varepsilon)}{\cos(\frac{\pi}{2} - a_S)}, \tag{1}$$

$$I_{dif,p} = I_{dif,h} \times \frac{1 + \cos(t)}{2} + A \times \left(I_{dir,h} + I_{dif,h}\right) \times \frac{1 - \cos(t)}{2}\Big) \tag{2}$$

$$\varepsilon = \arccos(\sin(\beta) \times \cos(t) + \cos(\beta) \times \sin(t) + \cos(a_P - a_S)) \tag{3}$$

Second, the incoming irradiance on the panel $I_{tot,p}$, i.e. the sum of direct and diffuse in-panel irradiance, is transformed to electrical power with a relative PV performance model by Huld et al. [20]. This model calculates the instantaneous efficiency (η_{rel}) relative to the efficiency at Standard Test Conditions (STC), which are defined as $T_{STC} = 25\,^{\circ}\mathrm{C}$ (standard cell temperature), $I_{tot,pSTC} = 1000\ \mathrm{W\,m^{-2}}$ (standard horizontal solar irradiance) and 45° (solar irradiance angle), for which the power output is known. The performance model takes the ambient temperature, the heating the panel experiences through incoming radiation and several coefficients depending on the chosen panel technology into account. In this study the values for Crystalline Silicon (c-Si) were used since it is the most common semiconducting material used for PV systems.

The sensitivity of PV electricity production to irradiance and ambient temperature, as modelled by GSEE, is illustrated in Fig. 1. As can be seen (Fig. 1b), the relative efficiency decreases linearly with increasing ambient temperature by approximately $-0.46\%\,^{\circ}\mathrm{C}^{-1}$, similar to values found in literature [1,25], and also decreases with increasing irradiance G, once the latter exceeds 200–300 $\mathrm{W\,m^{-2}}$. In contrast to ambient temperature, the sensitivity towards the in-panel irradiance is regarded as non-linear (Fig. 1a), with maximum efficiency at approximately ~ 400 $\mathrm{W\,m^{-2}}$. However, the non-linearity mainly affects η_{rel} for an irradiance up to the maximum. Above this level, η_{rel} decreases linearly, however with a shallow slope. Hence the non-linearity of GSEE mainly affects days with low irradiance, which predominantly occur in winter months throughout the whole day and during the sunrise and sunset period on all days of the year.

2.2. CMIP5 climate model data

We use CMIP5 for the prediction of future climate. In terms of climate change scenarios, RCP4.5 and RCP8.5 were considered, with RCP8.5 being the strongest climate change scenario. For the processing with the PV generation model, two variables of CMIP5 were required: surface downwelling shortwave radiation or all-sky shortwave radiation (*rsds*) and near-surface air temperature (*tas*). *rsds* aims to simulate realistic surface irradiances and thus includes effects of cloud cover and atmospheric composition on the magnitude of the surface radiation. This choice in variables resulted in a total number of 28 and 31 climate models available for RCP4.5 and RCP8.5, respectively.

Two 20-year time spans were examined for both RCP scenarios, to compare present and future PV potential. The first time span covers 2007–2027, forming a present reference period, while the second time span covers the future period from 2060 to 2080. The studied area is a rectangle covering Europe, spanning from −10° to 42° E and 30°–65° N. The CMIP5 data were available in monthly and daily temporal resolution. Both were used in the subsequent analysis to find a suitable setup to process the CMIP5 data with GSEE.

In order to reach a consistent set of climate model scenarios to compare, not all model outputs available in CMIP5 were used, some had to be excluded. Several of the mentioned 28 to 31 climate models (BCC-CMS1-1 and BCC-CMS1-1-m, IPSL-CM5A-LR and IPSL-CM5A-MR, MPI-ESM-LR and MPI-ESM-Mr) have multiple versions, the only difference being the spatial resolution (LR: low resolution,

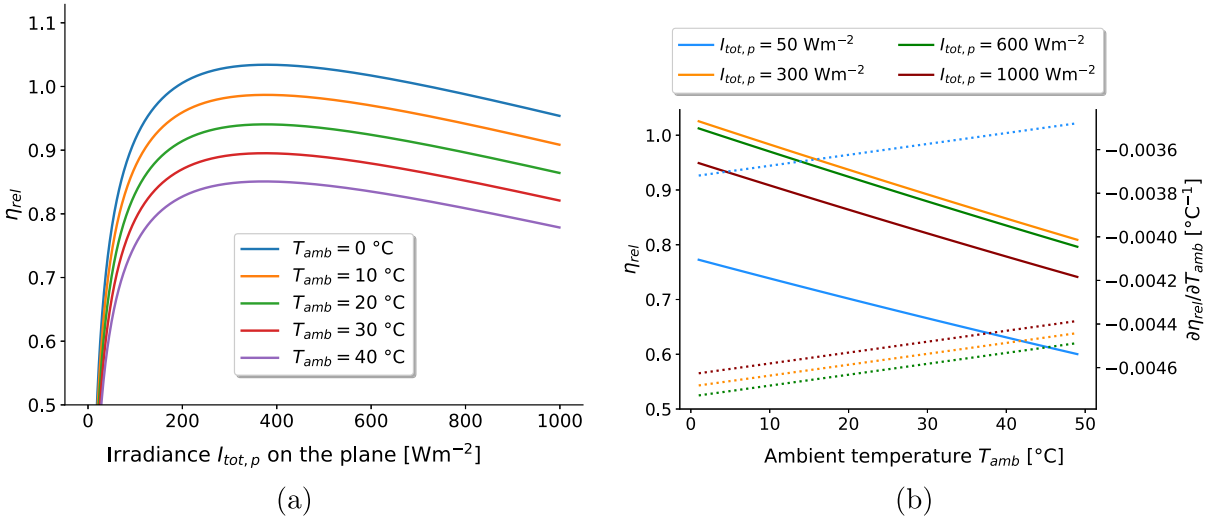

Fig. 1. GSEE sensitivity towards ambient in-panel irradiance and temperature. (a): Absolute η_{rel} depending on T_{amb} for different levels of irradiance. Typical horizontal irradiances on clear days lie between 300 and 500 $\mathrm{W\,m^{-2}}$/600–1000 $\mathrm{W\,m^{-2}}$ in winter/summer and between 50 and 150 $\mathrm{W\,m^{-2}}$/100–300 $\mathrm{W\,m^{-2}}$ on cloudy, foggy days. (b): Absolute η_{rel} (straight lines) and $\partial\eta_{rel}/\partial T_{amb}$ [%W^{-1}m^2] (dotted lines) as a function of ambient temperature (T_{amb}) for different in-panel irradiances ($I_{tot,p}$) [W m^{-2}]. Note that η_{rel} is 1.0 at standard test conditions, i.e. 25° C module temperature, but module temperature is always higher than ambient temperature due to the module heating coefficient, so efficiency is < 1.0 through most of the figure [20].

MR or -m: moderate resolution; [3,11]). For IPSL-CM5A and MPI-ESM the similarities between their versions with different resolution was shown by Ref. [26]. In order to avoid a bias towards these models, of each model only the version with the higher resolution was included in subsequent simulations. Knutti et al. [26] also show a strong similarity between MIROC-ESM and MIROC-ESM-CHEM, as they are essentially the same model except that MIROC-ESM-CHEM includes an atmospheric chemistry model [34]. GFDL-ESM2G and GFDL-ESM2M are also very similar, varying in the use of a different physical ocean component only [9]. Additionally, due to an inconsistency between the monthly and daily mean data, the models BNU-ESM and CCSM4 were omitted (See supplementary material). Hence 21 and 23 climate models (Table 1) for RCP4.5 and 8.5, respectively, were left for the estimation of future PV electricity yield. Projections for *rsds* and *tas* can be found in the supplementary material.

Table 1
CMIP5 models providing daily mean data. Listed are models that provide both variables *rsds* and *tas* in daily resolution for the RCPs 4.5 and 8.5. Also depicted is their spatial resolution (in °latitude (*lat*) and °longitude (*lon*)) as well as the responsible modelling groups and countries [12].

Modelling group (Country)	Name	Atmospheric Grid		RCP	
		lat	lon	4.5	8.5
CISRO-BOM (Australia)	ACCESS1.0	1.25	1.875	•	•
	ACCESS1.3	1.25	1.875	•	•
BCC (China)	BCC-CMS1-1-m	1.125	1.125	•	•
CCCMA (Canada)	CanESM2	2.7906	2.8125	•	•
CMCC (Italy)	CMCC-CESM	3.4431	3.75		•
	CMCC-CM	0.7484	0.75	•	•
	CMCC-CMS	3.7111	3.75	•	•
CNRM-CERFACS (France)	CNRM-CM5	1.4008	1.40625	•	•
CISRO (Australia)	CISRO-Mk3.6.0	1.8653	1.875	•	•
NOAA GFDL	GFDL-CM3	2	2.5	•	•
(USA)	GFDL-ESM2G	2.0225	2	•	•
NIMR/KMA	HadGEM2-AO	1.25	1.875	•	•
INM (Russia)	INM-CM4	1.5	2	•	•
MOHC (United Kingdom)	HadGEM2-CC	1.25	1.875	•	•
	HadGEM2-ES	1.25	1.875	•	•
IPSL (France)	IPSL-CM5A-MR	1.2676	2.5	•	•
	IPSL-CM5B-LR	1.8947	3.75	•	•
MIROC (Japan)	MIROC-ESM-CHEM	2.7906	2.8125	•	•
	MIROC5	1.4008	1.40625	•	•
MPI-M (Germany)	MPI-ESM-MR	1.8653	1.875	•	•
MRI (Japan)	MRI-CGCM3	1.12148	1.125		•
	MRI-ESM1	1.12148	1.125	•	•
NCC (Norway)	NorESM1-M	1.8947	2.5	•	•

To disentangle the effect of changes in cloudiness or aerosol composition on the total irradiance we use monthly data on clear-sky shortwave radiation (*rsdscs*) in addition to *rsds* and *tas*. The change in *rsdscs* between the present and the future time period was regarded as the change in *rsds* caused by alterations in atmospheric composition and the difference between *rsdscs* and *rsds* as the change in the amount of radiation clouds absorb or scatter. With this data we estimate the fraction of changes in *rsds* due to changes in cloud properties.

According to Wild et al. [35] the CMIP5 models are mostly consistent in the sign of projected change in terms of *rsds* and *tas* over the most part of Europe. Generally, the robustness and uncertainties of the CMIP5 dataset is discussed by Ref. [26].

2.3. Processing CMIP5 data with GSEE

The processing chain from CMIP5 model data to GSEE modelled PV electricity output is schematically given in Fig. 2. It shows that GSEE calculates PV electricity output on an hourly basis and thus requires its input variables (total horizontal irradiance, diffuse fraction, temperature) to be in hourly resolution as well. However, CMIP5 models and most observational records only provide daily means of radiation and temperature data, which are insufficient for accurate PV electricity simulations. A PV panel's angle of incidence strongly depends on the time of day, which directly affects the amount of direct radiation reaching the panel. Additionally, the diffuse fraction is closely related to the solar altitude angle and thus the hour of the day. These two facts, together with the non-linearity of the PV system, make the use of at least hourly resolution data for irradiance a necessity for accurate calculations of daily PV electricity output. For this study we derive hourly irradiance values with an artificial diurnal cycle following a sinusoidal function, depending only on the total horizontal incoming irradiance ($I_{tot,h}$), and sunrise (S_r) and sunset hours (S_s) (Eq. (4)). This diurnal cycle produces a first-order approximation of the course of total irradiance on a clear-sky day. To calculate PV output with monthly mean data, the model is run once for a day in the middle of the month, serving as a representative for the whole month.

$$I_h = \sin\left(\frac{\pi}{dt} \times (h - S_r)\right) \times \frac{I_{tot,h}\pi}{2dt}, \quad dt = S_s - S_r \tag{4}$$

The CMIP5 data does not include diffuse irradiance or diffuse fraction as a variable. Solely the sum of direct and diffuse radiation, surface downwelling shortwave radiation (*rsds*), which equals the

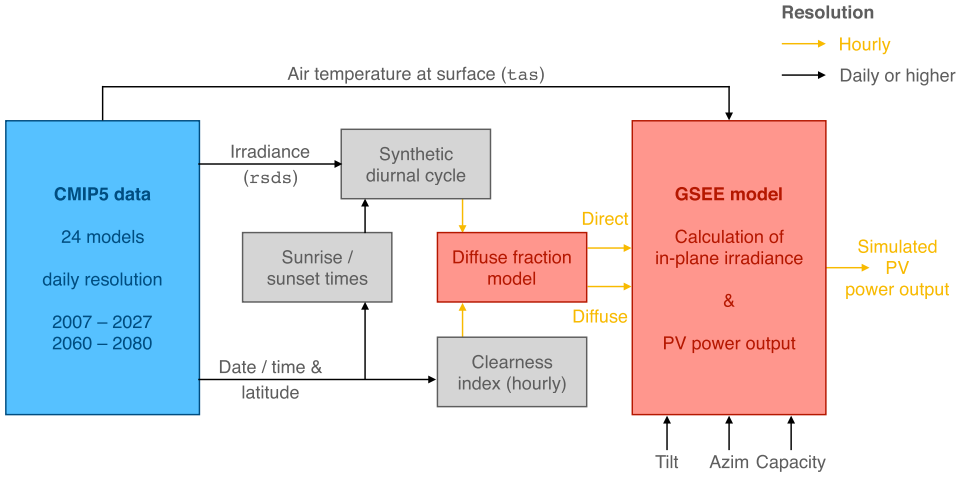

Fig. 2. Schematic showing the structure of how the CMIP5 data and GSEE model are coupled. All code is available as a submodule of GSEE (https://pypi.org/project/gsee/).

total horizontal irradiance required by GSEE, is available. Thus it was necessary to estimate the diffuse fraction from the total horizontal irradiance with a semiempirical model, the Boland-Ridley-Lauret (BRL) model [30]. Several other models to estimate the diffuse fraction exist. All of them make use of the hourly (k_t) and daily (K_t) atmospheric clearness indices [8], which are calculated following the equations from Ref. [10]. The BRL model is superior for two reasons. First, it uses additional parameters (*AST* apparent solar time; a_s solar elevation; ψ persistence index) to the hourly and daily clearness index to calculate the diffuse fraction k_d. Second, it is regarded as a globally applicable model [30] and has empirically proven to be among the best models to estimate diffuse fraction [32].

For ambient temperature it was sufficient to use the daily mean value across all hours of the day. This did not introduce significant enough error to justify the computational overhead caused by the implementation of an additional diurnal temperature cycle. The uncertainty of this approach to use daily data, compared to the optimal case where hourly data is available, is presented in Sect. 3.3.

For each of the climate models, output for *rsds* and *tas* was processed with GSEE for both a present (2007–2027) and future (2060–2080) time period as well as both RCP scenarios 4.5 and 8.5. To deal with the different spatial resolutions of the models, the resulting datasets on PV electricity generation potential were remapped bilinearly to a common grid of 29 × 30 cells over Europe with a resolution of 1.25 × 1.875°. This grid is the same as used by ACCESS1.0 and 1.3 and is of an average resolution when compared with the bulk of models. All calculations simulate one single panel per grid cell with an azimuth of 180° (southwards), capacity of 1 kW (maximum possible output) and no tracking enabled. The tilt angle was calculated individually for each latitude, following a linear regression (Eq. (5)).

$$tilt = 0.35396 \times lat + 16.84775 \quad (5)$$

This relationship is derived from estimates for optimal tilt angles for 54 stations in Europe [23] and serves as an estimate for optimal tilt in this study. There are several other simple tilt angle-latitude relations used as rule of thumb by solar energy system installers [37], thus this slightly more sophisticated relationship (Eq. (5)) should serve as an adequate estimate of PV systems installed in reality. All resulting PV projections were analysed individually and the ensemble mean taken to summarise the results. The resulting code is published as a submodule to GSEE (https://pypi.org/project/gsee/).

2.4. European energy scenario

Results from the methods presented up to this point were used to determine the future PV electricity generation potential in Europe. Of course these results only matter for regions where PV systems do or will exist. Currently, there are large differences in the national electricity generation mix of different European countries as well as in electricity demand. Such differences will likely still be present in the future European energy system. Therefore, the impact of climate change will affect each country differently. In order to demonstrate these individual impacts, we use the European Commission's reference 2050 energy scenario and determined how climate change (prescribed by RCP8.5) would affect the PV electricity generation component of this scenario. The scenario cannot be considered a forecast, but rather as a trend projection. It is guided by the legally binding GHG and Renewable Energy Sources (RES) targets of the EU and assumes all policies up to 2014 to be implemented [5]. Scenario data are available for all EU-27 countries.

The energy system scenario provides information on the net generation capacity of PV, the gross electricity generation of the whole energy system and the share of electricity produced from PV for the present and up to the year 2050. Together with the projections of PV electricity generation potential in this study, this allowed us to estimate the impact climate change may have on these future European energy systems. For each country the climate change impact was calculated by averaging each grid cell whose centre is located in the corresponding country's borders. This impact multiplied with the country's share of potential future PV production provides information on how different European countries with their individual electricity generation mix may be affected by climate change.

2.5. CM-SAF SARAH and MERRA-2 historical weather data

To develop the method (Sect. 2.3) for the processing of CMIP5 data with the GSEE we use surface incoming shortwave radiation (*sis*) and direct normalised irradiance (*dni*) from the satellite based SARAH and temperature at 2 m above displacement height (*t2m*) from the MERRA-2 dataset for the years 2011–2015 in hourly resolution and spatial resolutions of 0.05° × 0.05° and 0.5° × 0.66°, respectively. We use a subsample of both datasets consisting of locations distributed across Europe in the form of a 2° × 2° grid. This results in 163 homogeneously distributed, land-based sample locations in Europe. For all locations the fraction of incoming horizontal diffuse radiation was calculated with *dni* and *sis*, from SARAH, and the sun's local zenith angle for the entire time period of 2011–2015 in hourly resolution. The locations were used to determine the uncertainty introduced depending on the choice of temporal resolution of the initial radiation and temperature data as well as the method of upsampling of CMIP5-based daily radiation data to hourly values. As both SARAH and MERRA-2 are available in hourly resolution and together deliver both temperature and irradiance, they fulfil the input requirements for GSEE model.

3. Results

We first turn to projected changes in potential PV electricity production (Sect. 3.1), which we then combine with a scenario of future PV installations (Sect. 3.2). Uncertainties associated with the necessary pre-processing of the CMIP5 data are quantified (Sect. 3.3) and the relative importance of changes in temperature and irradiance (Sect. 3.4) as well as potential physical causes (Sect. 3.5) are examined. We show only figures based on RCP8.5. Results for RCP4.5 are in the supplementary material.

3.1. PV projections

We show the total yearly production of the present (2007–2027) time period based on CMIP5 data and GSEE in Fig. 3a. In the future (2060–2080) time period, results show that PV electricity production is changed by the percentage shown in Fig. 3b, ranging from −6% to 3%. The region of strong increase follows roughly European land masses, up to about 55° N in the west but only up to about 45° N in the east. Beside the magnitude of change, the possibility of changes in variability is of interest. In regions which will potentially rely heavily on solar power in the future, a change in variability would affect the extent to which solutions to balance variability, such as storage, are required. In Fig. 3c we show the ensemble mean of the relative change between the present and future in intra-annual variance (i.e. seasonal) over the entire 20-year time period, based on the calculated daily means of PV potential. Two distinct regions of interest are identifiable. The first is

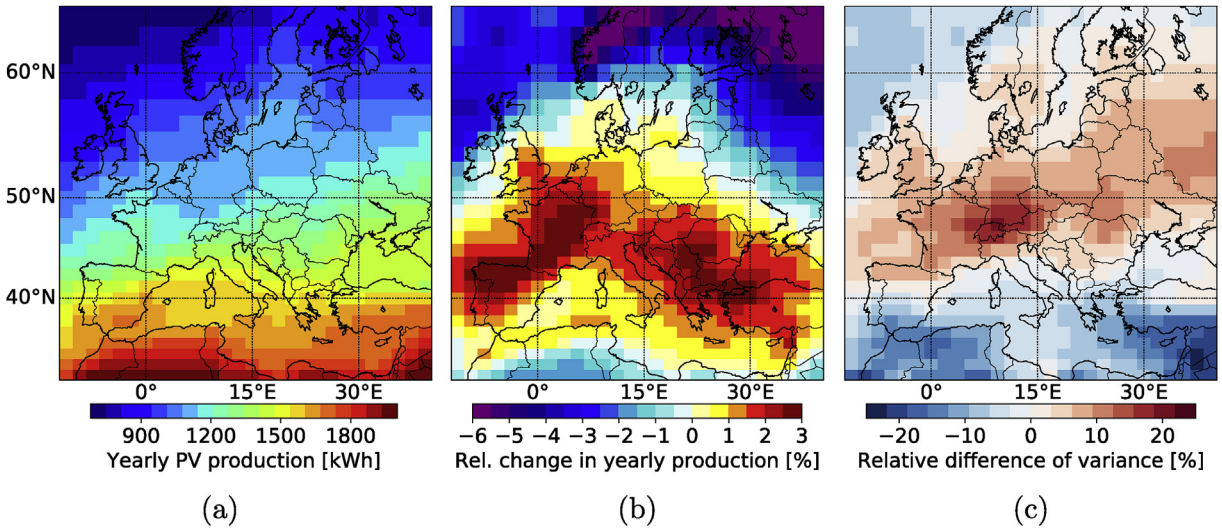

Fig. 3. Results for present yearly total PV potential and future relative change and variance compared to the present under the RCP8.5 climate change scenario. Maps show the ensemble mean of the CMIP5 models of the total PV potential (**a**) for the present (2007–2027), (**b**) relative difference in yearly sum of produced power, and (**c**) intra-annual (seasonal) variance between the present (2007–2027) and future (2060–2080) time periods.

Europe above 40° N with a hot spot in southern Germany, where an increase in variance over the whole year is expected. The second region is below 40° N, where variance decreases in general. In both directions the change in variance lies in the range of up to ± 20%. This means the peaks in production throughout the year will drift further apart or together for the regions with increased or decreased intra-annual variance, respectively.

Since PV electricity production (and electricity consumption) are strongly dependent on season, it is worthwhile to examine the change patterns of Fig. 3b and c on a monthly mean scale, shown in Figs. 4 and 5. Fig. 4 shows the multi-year average relative change in PV potential between the present and future time periods on a

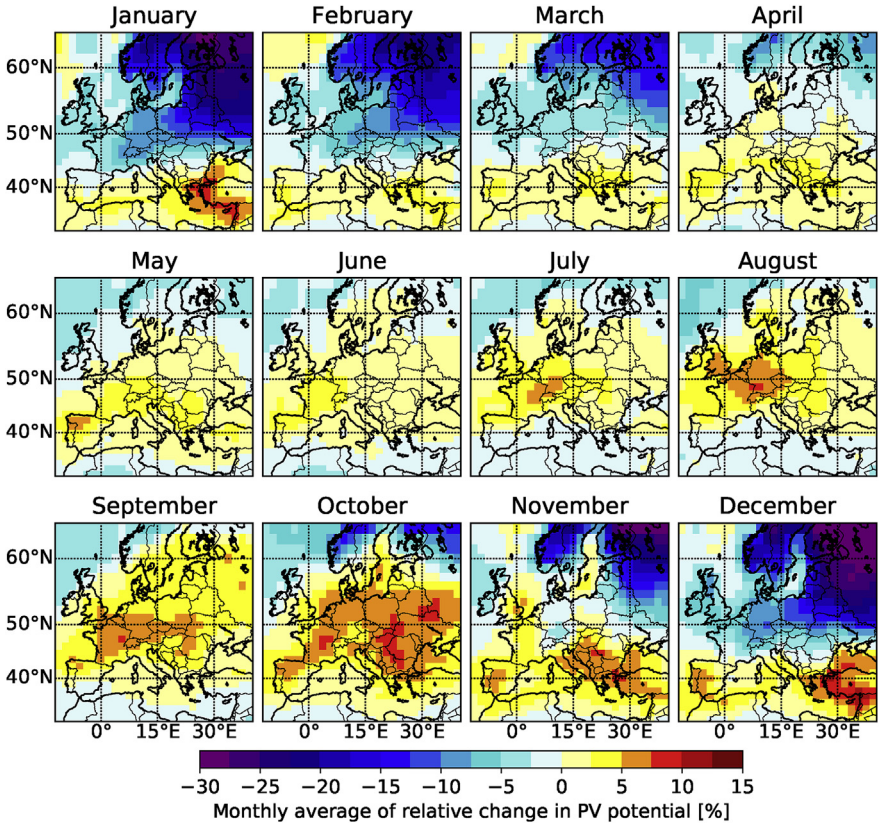

Fig. 4. Projection of monthly relative change in PV potential under scenario RCP8.5 compared to the present. Maps show the average relative increase or decrease in potential PV electricity production. They are composed of the ensemble mean of all CMIP5 models for which we calculated the difference of the monthly multi-year average between the present (2007–2027) and future (2060–2080) time periods individually. Positive/negative values indicate an increase/decrease of PV electricity output in the future.

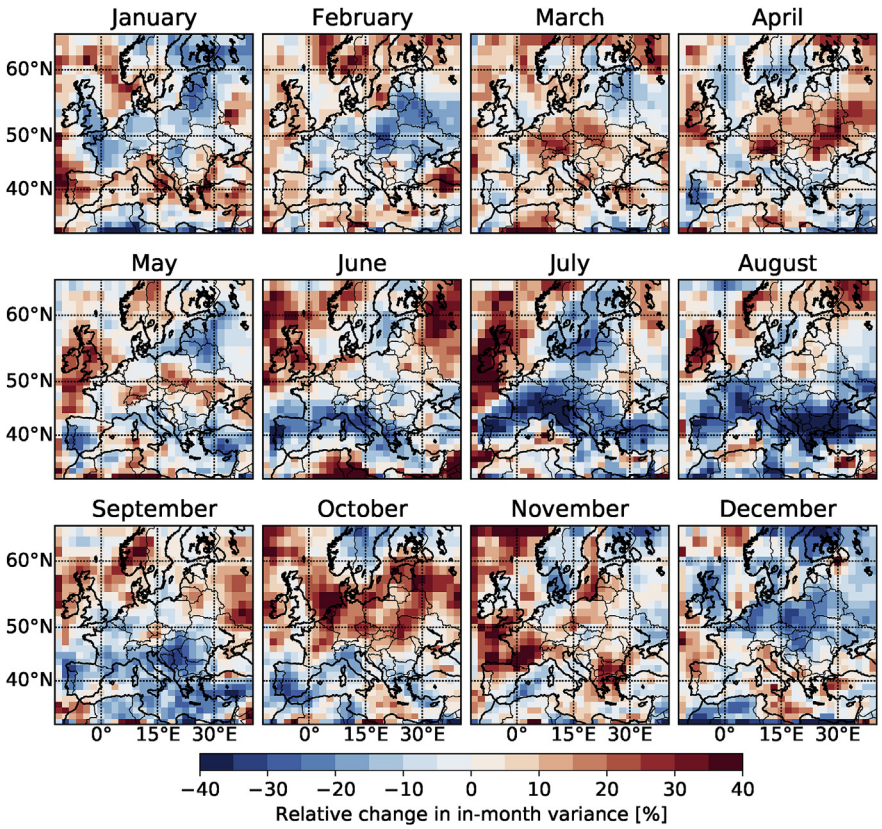

Fig. 5. Changes in multi-year monthly variance in PV electricity generation compared to the present. The maps show the ensemble mean of the CMIP5 models of the relative difference in multi-year monthly variance between the present (2007–2027) and future (2060–2080) time periods for RCP8.5, i.e., the variance for each month was calculated separately. The variance is calculated over both time spans with monthly mean data of PV electricity generation.

monthly basis. The largest relative change is observed in north-eastern Europe (Russia, Scandinavia, the Baltic states, and Finland) during winter months (−30%). Central Europe also experiences a reduction of PV potential in winter, however only in the range of −10%, while in the south-eastern Mediterranean we observe an increase in PV potential. The largest positive changes can be found in central and south-eastern Europe, during the summer and especially in the autumn months (+10%). While the large negative changes in relative terms in north-eastern Europe may seem to suggest that the PV potential reduction is larger there, in absolute numbers the changes are on a similar level as elsewhere in Europe. However, at high latitudes, where the absolute PV potential is small particularly in winter, this results in a higher relative change.

Examining the variability in monthly means in Fig. 5, it is evident that in central Europe the variance between seasons will decrease in winter and summer and increase in the transitional months of autumn and spring. Around the British Isles, variance increases in the summer months. It also increases in some parts of the Mediterranean in December and January. The strongest decrease in variance can be found along the northern coast of the Mediterranean in July and August.

In order to test the robustness of the observed shifts in the mean of the PV potential, we perform a two-sided *t*-test with a significance level of 0.05, comparing the PV potential of the two time periods for RCP8.5 with a null hypothesis of equal means. The test was done separately for each month with the calculated daily mean of PV potential. Fig. 6 shows the results of this test. The blue and red areas show the grid points where a majority of CMIP5 models (fraction of models > 0.5) show a significant decrease and increase in PV potential, respectively. The darker the colour, the larger the fraction of models that show the same or lower level of significance. We observe both significant increases as well as decreases in PV potential throughout the year. The *t*-test shows that the negative changes in winter months, especially in the Scandinavian and Baltic states as well as Belarus and Russia, are of statistical significance. Significant positive changes are observed in the regions north and east of the eastern Mediterranean basin in winter and in northern Spain, France and central Europe in summer. Spring and autumn show a transition period between the states of winter and summer, with only few and scattered regions of significant change. This is consistent with the results from Ref. [16], which showed that the probability that changes in radiation are solely due to internal variability is very low.

3.2. Impact on future energy system

We have shown the impact of climate change on PV electricity generation potential in Europe. Of course, this impact is of no interest if no PV infrastructure exists to be affected. Fig. 7 shows how the future European energy system specified by the European Commission's reference 2050 energy scenario [15] may be affected by climate change, both as relative change of country-wide PV generation and as absolute effect on a country's total electricity generation. Over the whole of central a southern Europe, we see increased electricity yields. This is primarily because PV systems in countries including Spain, France, Italy and Germany are expected to yield additional electricity. These are also the countries where most of Europe's future PV capacity is expected to be. Even though our results show a significant reduction in PV electricity generation

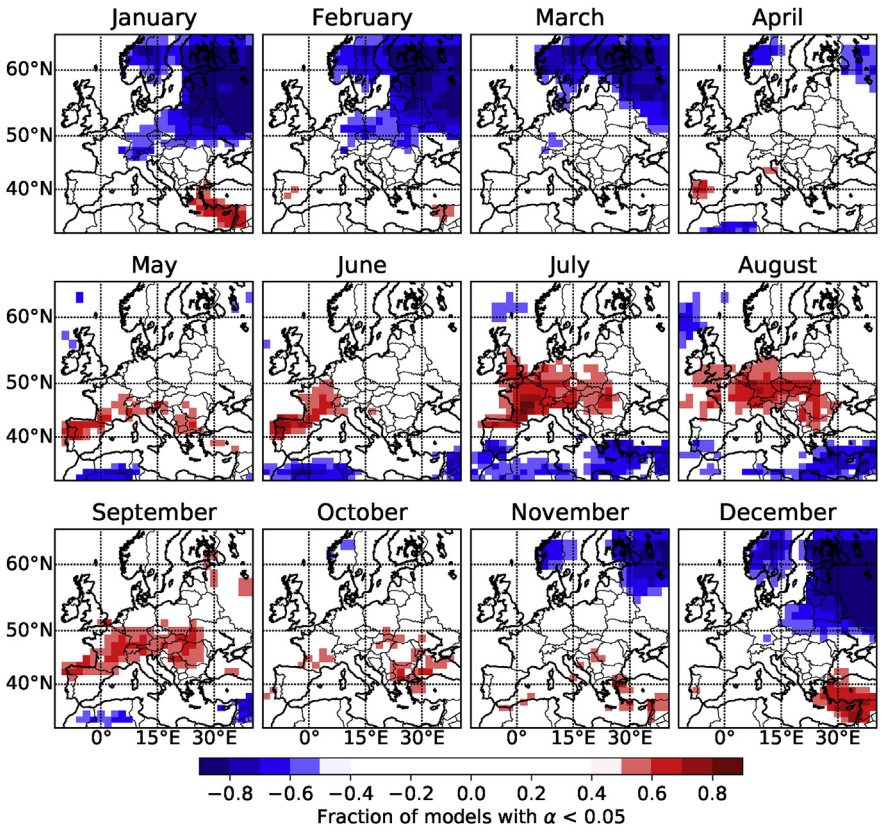

Fig. 6. Regions with statistically significant change in PV power production for RCP8.5. Maps highlight the locations where the majority of the CMIP5 climate models show an increase or decrease in the potential PV electricity production with a significance level below 5% in a two-sided *t*-test. The values indicate the fraction of models that agree on this significance, while positive or negative values stand for a significant increase or decrease, respectively. The significance was tested with daily data for each month, comparing the present (2007–2027) and future (2060–2080) time periods.

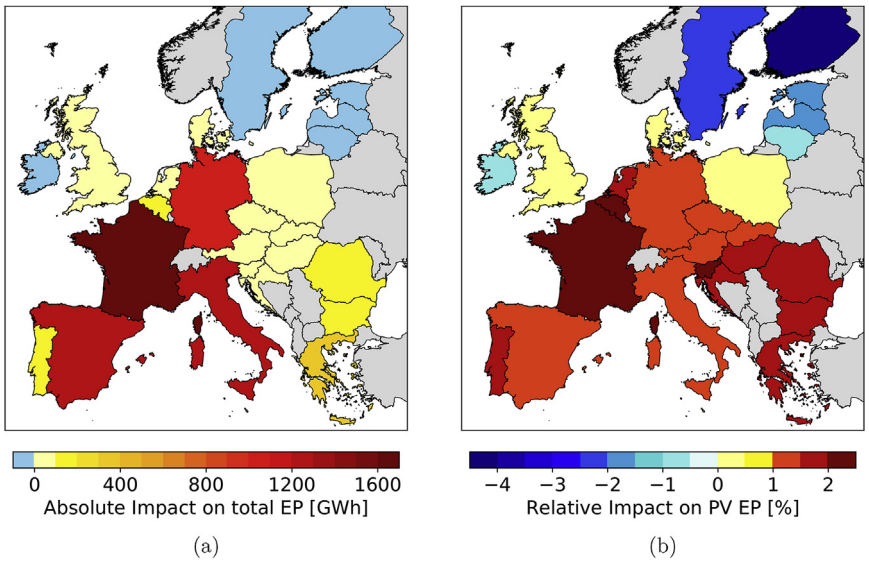

Fig. 7. Absolute (a) and relative (b) impact of climate change on the EU PV installation projection. The maps show (**a**) absolute in GWh and (**b**) relative impact of climate change (with RCP8.5) on the PV electricity generation projections for the European Commission's 2050 reference scenario [15]. Countries shaded in black are those where no data on installed PV capacity are available.

potential in the northern regions of Europe, these regions are not expected to deploy large PV fleets, so the effect of this reduction on the European energy system as a whole is small. Instead, Europe as a whole may gain up to 6.52 TWh/yr of additional electricity generation from PV, solely through the effects of climate change. By taking the projections for on *average cost of gross electricity generation* and *average price of electricity in final demand sectors* for each country from Ref. [15], this would result in an additional profit of

581 million per year for PV system operators Europe-wide.

3.3. Sensitivity to time resolution and upsampling methods

The GSEE model takes hourly values of radiation, diffuse fraction, as well as temperature as input (see Sect. 2.1). Data at that resolution are, however, not always available. For example, model or observational data may come only as monthly mean values. Consequently, assumptions have to be made on how to relate the available data to the hourly data required by GSEE. In the following we quantify the uncertainty range of the PV potential depending on the temporal resolution of the input data to GSEE and the targeted resolution of PV potential. To this end, we started from hourly radiation and temperature data from SARAH and MERRA-2, which we re-aggregated into daily, monthly, seasonal, and annual data. Results from running GSEE on the original hourly data served as our benchmark, against which we compared the results from simulations with GSEE and the re-aggregated data. The resulting deviations are aggregated over the 163 individual geographical locations considered (Sect. 2.5) while being divided into northern and southern European locations at 50° N. Finally, we show that a sinusoidal diurnal cycle (as described in Sect. 2.1) is clearly superior to uniformly distributing the radiation over the day. All figures show the relative deviation as well as the absolute deviations normalised by the yearly average in PV production.

Fig. 8 shows the mean deviations and uncertainties introduced by calculating monthly PV potential with monthly or daily mean data compared to the output from hourly radiation and temperature data. PV yield from monthly data was calculated by assigning the monthly mean to the central day of the month, simulating this

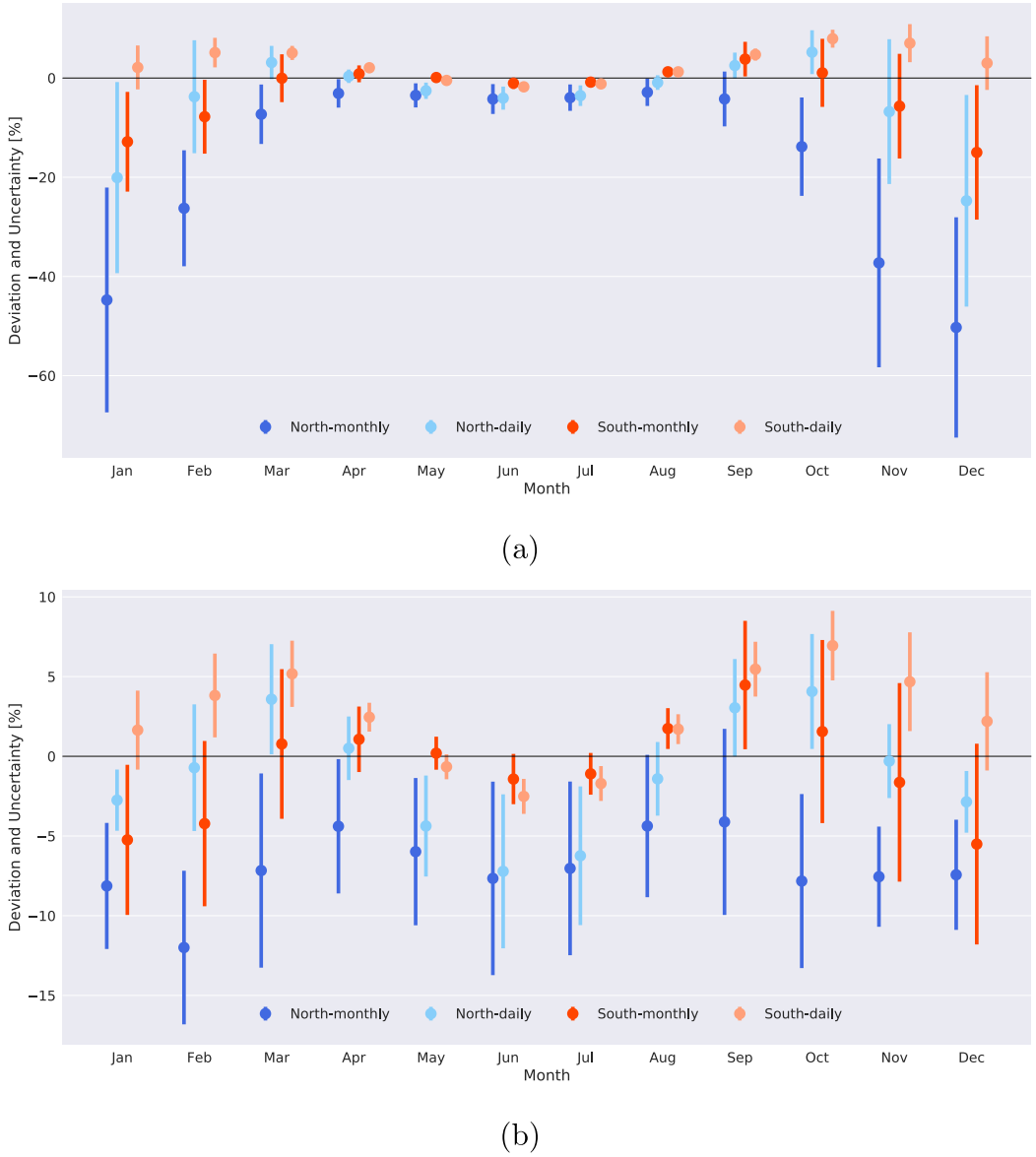

Fig. 8. Error bars showing the relative (a) and absolute (b) deviation of monthly PV production data based on the temporal resolution of the input data (*rsds*, *tas* in monthly or daily resolution) and the latitude (northern or southern Europe) compared to the benchmark PV production calculated from hourly data. The absolute deviation is normalised by the yearly average in PV production. The dot represents the average deviation and the bars enclose one standard deviation in both directions. Blue shows the deviation and uncertainty for northern locations (above 50° N) and monthly initial data, light-blue for northern locations and daily data, red for southern locations and monthly data and light-red for southern and daily data, respectively. (For interpretation of the references to colour in this figure legend, the reader is referred to the Web version of this article.)

day with GSEE and considering the result as the average monthly PV yield. From Fig. 8 we can conclude that using input data in monthly mean resolution generally underestimates PV yield, especially in the winter months and northern locations, yet in absolute terms, the deviation in winter and summer are similar. Additionally the uncertainty of the deviation is larger for calculations based on monthly mean data and locations in the north.

The results when using monthly input data can be strongly improved with the use of characteristic probability density functions for each month, describing the probability with which a day with a certain amount of radiation occurs (see example distributions in Fig. 9). With this additional information, using monthly data performs very similarly to the use of daily mean data (thus not included in Fig. 8. However, these probability density functions depend on local climate conditions and their shape likely varies substantially from region to region. Even at a given location, they may change through time due to internal variability or changes in climatology, possibly caused by climate change. Thus, the use of daily data is still superior as the internal distribution of radiation across the days of a month is included by definition.

Tables 2 and 3 show results of the same type as Fig. 8, if seasonal or annual PV electricity generation data should be achieved. Annual

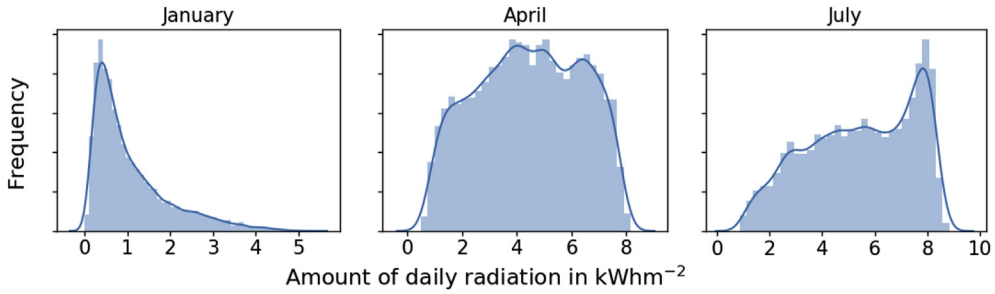

Fig. 9. Examples of monthly characteristic probability density functions of daily radiation values based on SARAH data, describing the probability of a day with a certain amount of radiation (x-axis) to occur (probability density functions for all months shown in supplementary material).

Table 2
Mean relative and absolute deviation and uncertainty for seasonal PV production data based on the temporal resolution of the input data (*rsds*, *tas* in seasonal, monthly or daily resolution) compared to PV production calculated from hourly data. The absolute error is normalised by the yearly average in PV production. Values are noted in percent as mean $\pm\sigma$ (standard deviation). Values are categorised in northern (above 50° N) and southern (below 50° N) locations.

Units: %	Seasonal input data		Monthly input data		Daily input data	
	relative	absolute normalised	relative	absolute normalised	relative	absolute normalised
North:						
Spring	−4.38 ± 3.35	−6.20 ± 4.94	−4.12 ± 2.67	−5.80 ± 3.96	−0.01 ± 1.67	−0.10 ± 2.39
Summer	−6.80 ± 2.93	−11.38 ± 5.77	−3.69 ± 2.67	−6.27 ± 4.97	−2.91 ± 1.89	−4.93 ± 3.57
Autumn	3.19 ± 8.69	2.66 ± 5.97	−10.27 ± 5.79	−6.48 ± 3.25	2.93 ± 3.16	2.29 ± 2.40
Winter	−21.47 ± 19.30	−5.15 ± 3.24	−31.96 ± 11.19	−8.06 ± 2.59	−10.33 ± 11.15	−1.95 ± 1.54
South:						
Spring	0.37 ± 2.13	0.34 ± 2.49	0.49 ± 1.65	0.56 ± 1.88	2.00 ± 0.75	2.32 ± 0.91
Summer	−2.90 ± 0.85	−3.91 ± 1.26	−0.24 ± 0.74	−0.35 ± 1.04	−0.57 ± 0.63	−0.82 ± 0.90
Autumn	8.74 ± 5.98	7.70 ± 5.33	1.21 ± 4.85	1.32 ± 4.20	6.46 ± 1.54	5.71 ± 1.66
Winter	−3.44 ± 10.65	−0.25 ± 6.50	−10.76 ± 8.19	−5.07 ± 4.14	3.56 ± 3.34	2.33 ± 2.21

Table 3
Mean relative and absolute deviation and uncertainty for annual PV production data based on the temporal resolution of the input data (*rsds*, *tas* in annual, seasonal, monthly or daily resolution) compared to PV production calculated from hourly data. The absolute error is normalised by the yearly average in PV production. Values are noted in percent as mean$\pm\sigma$ (standard deviation). Values are categorised in northern (above 50 N) and southern (below 50 N) locations.

Units: %		annual	seasonal	monthly	daily
relative and	*North:*	16.29 ± 7.80	−0.84 ± 9.67	−7.10 ± 2.56	−1.19 ± 2.02
absolute normalised	*South:*	10.25 ± 2.99	3.35 ± 6.52	−1.06 ± 2.34	2.42 ± 1.02

Table 4
Comparison of results with similar studies. The Table 4 compares the approximate results from Crook et al. [7], Wild et al. [35] and Jerez et al. [24] to the results attained in this study. Data was inferred from the figures reported in the respective papers and divided into several regions. The years in the column title show the year or timespan for which the data is given. The numbers show the percentage change in future average PV power output in those regions relative to the present as reported by these studies.

Regions	Crook et al. 2080 [%]	Wild et al. 2070 [%]	Jerez et al. 2070–2099 [%]	This study 2060–2080 [%]
Spain	2–6	1.6–4.3	−5 - 5	0.5–3
France	2–6	1.6–3.2	−5 - 0	1–3
Germany	4–8	0.5–3.2	−10 - 0	0.5–2.5
Central Europe	2–8	0–3.2	−10–−5	−0.5 - 2
South-eastern Europe	4–8	2.7–4.3	−5 - 0	1.5–3
North-eastern Europe	0–4	0	−10–−5	−4 - 0
Northern Europe	−2 - 2	0–0.5	−15–−10	−3 - 0

PV yield was calculated by simulating one day each in GSEE at the beginning of the 2nd and 4th quarter upsampled with a sinusoidal diurnal radiation cycle and averaging the result to represent the annual mean. Since the absolute values are normalised by the yearly mean in production, they equal the relative deviations in this case. Seasonal PV yields were calculated in the same manner as yields from monthly mean data, however with the representative day selected from the centre of each season instead of each month. Monthly data is again based on one central representative day. From Table 3 we conclude that when targeting an annual resolution of output data from northern locations, at least seasonal input data should be used. However, monthly input data lead to an additional reduction in the uncertainty of the results. Targeting seasonal data (Table 2) is more complex. Depending on the season the deviations and uncertainties vary strongly. For example, in winter, seasonal and monthly input data strongly underestimate the PV yield, with high uncertainties, while in spring and summer, monthly input data may suffice for adequate prediction of seasonal PV yield.

In Fig. 10 the deviations and uncertainties introduced by using two approaches of how the sum of radiation can be distributed among the hours of the day is shown. In addition to the sinusoidal distribution of radiation used in this study a simpler method was evaluated. It distributes the sum of radiation uniformly among the hours between sunrise and sunset of each day. As expected, the method to sinusoidally distribute radiation introduces less uncertainty throughout the year when compared to the reference. For the largest part, this can be explained by trigonometry and the non-linear response of a PV electricity output to irradiance as

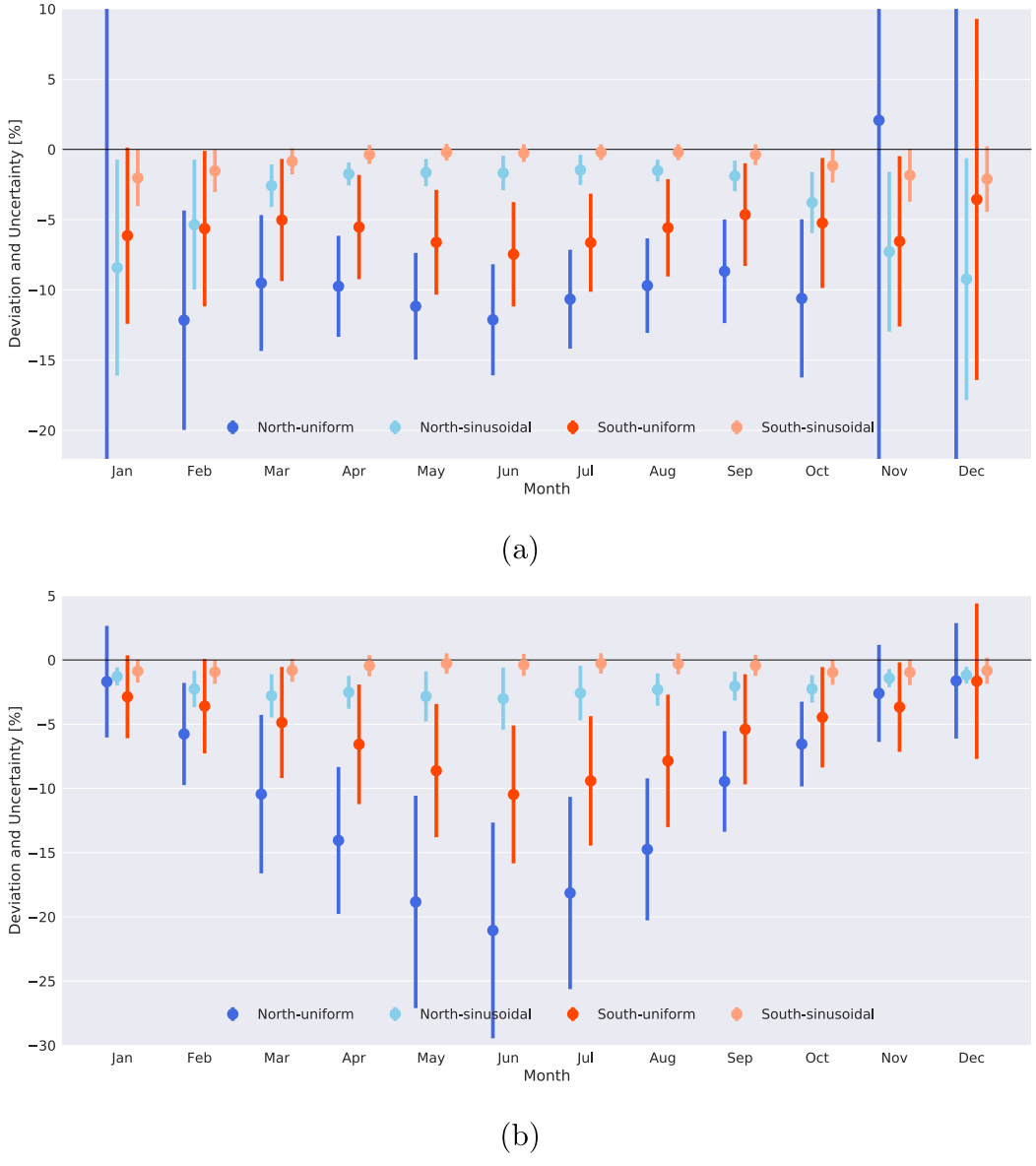

Fig. 10. Error bars showing the relative (a) and absolute (b) deviation of monthly PV production data based on the method of upsampling *rsds* to hourly values compared to PV production calculated from initially hourly data. The absolute error is normalised by the yearly average in PV production. The dot represents the average deviation and the bars enclose one standard deviation in both directions. Blue shows the deviation and uncertainty for northern locations (above 50° N) and uniformly, light blue for northern locations and sinusoidally, red for southern locations and uniformly and light red for southern and sinusoidally distributed radiation, respectively. For visibility reasons (a) does not show the whole error bar for January, November, December for *North-uniform*, however the figure is also represented as a table in the supplementary material. (For interpretation of the references to colour in this figure legend, the reader is referred to the Web version of this article.)

modelled by GSEE. Since almost all PV panels are tilted, the energy input into a panel depends on the angle of incidence (i.e., how much radiation hits the surface of a panel). Because the angle of incidence changes throughout the day, PV electricity output depends on the hour at which the radiation reaches the panel. The error is generally larger in winter, which is mainly caused by the overall lower absolute PV electricity production. Because of its large impact on accuracy, the simple sinusoidal diurnal cycle model was considered a mandatory addition to the CMIP5-GSEE setup used.

3.4. Sensitivity to temperature and irradiance

The estimated changes in PV electricity generation in the future are the product of changes in irradiance and temperature. Fig. 11a and b shows the resulting PV potential from a run with GSEE where only one of the two climatological variables (either *rsds* or *tas*) was taken from the future (2060–2080) period, while the other was left at the state of the present period (2007–2027). This shows how strongly the two variables contribute to the change in PV potential between the present and the future. Generally, the majority of climate change impact on PV potential is caused by changes in irradiance, while an increase in temperature reduces PV electricity output with a magnitude of 1–2%. On the one hand, in central Europe and the south-eastern Mediterranean during late summer and winter, respectively, the increase of temperature leads to a dampening of higher generation induced by the increase in radiation. On the other hand, in the northern regions, the reduction in PV generation induced by the radiation decrease is reinforced by the simultaneous negative effect of rising temperatures.

As GSEE is characterised by a nearly linear relationship between ambient temperature and relative efficiency, the temperature increase caused by climate change affects PV yield (relatively) homogeneously and proportionally to the temperature change. In contrast, due to the non-linearity of the relationship between irradiance and relative efficiency, i.e. the disproportionately low relative PV efficiency at low levels of irradiance, a region characterised by a decrease in irradiance experiences an even stronger decrease in PV potential.

3.5. Changes in cloud cover and atmospheric composition

The change in irradiance in the future can be further split into changes caused by a shift in extinction through clouds and changes in atmospheric composition. Fig. 12a shows the fraction of overall change in irradiance between the present and future time period caused by changes in cloud effects (difference between *rsds* and *rsdscs*). It follows that the remaining change in irradiance is due to changes in the composition of the atmosphere (aerosols, water vapour, greenhouse gases). Across almost all of Europe, changes in clouds are responsible for the majority of change in *rsds*. Especially around central Europe during the warmer half of the year the fraction goes up to 80%. These two effects, the changes in cloudiness and atmospheric composition, together explain almost all of the change in *rsds* from present to future. When summed up over all of Europe, they predict *rsds* with an average relative error of +1.92% and a standard deviation of the error of 2.08%.

4. Discussion and conclusion

We use daily radiation and temperature data from 23 CMIP5 climate models and two emission scenarios (RCP4.5 and 8.5) to estimate monthly PV potential for a present (2007–2027) and future (2060–2080) time period in Europe. We present several options on how monthly or daily climate model data can be processed with an hourly PV electricity generation model and provide information on data requirements, in terms of resolution, to achieve accurate results for the electric power output of a PV panel with input data at less than hourly resolution. Comparing the present and future time periods, for a scenario of strong climate change (RCP8.5), we show a significant increase in PV electricity generation potential around central Europe in summer and a decrease in northern regions in winter. The change in PV potential

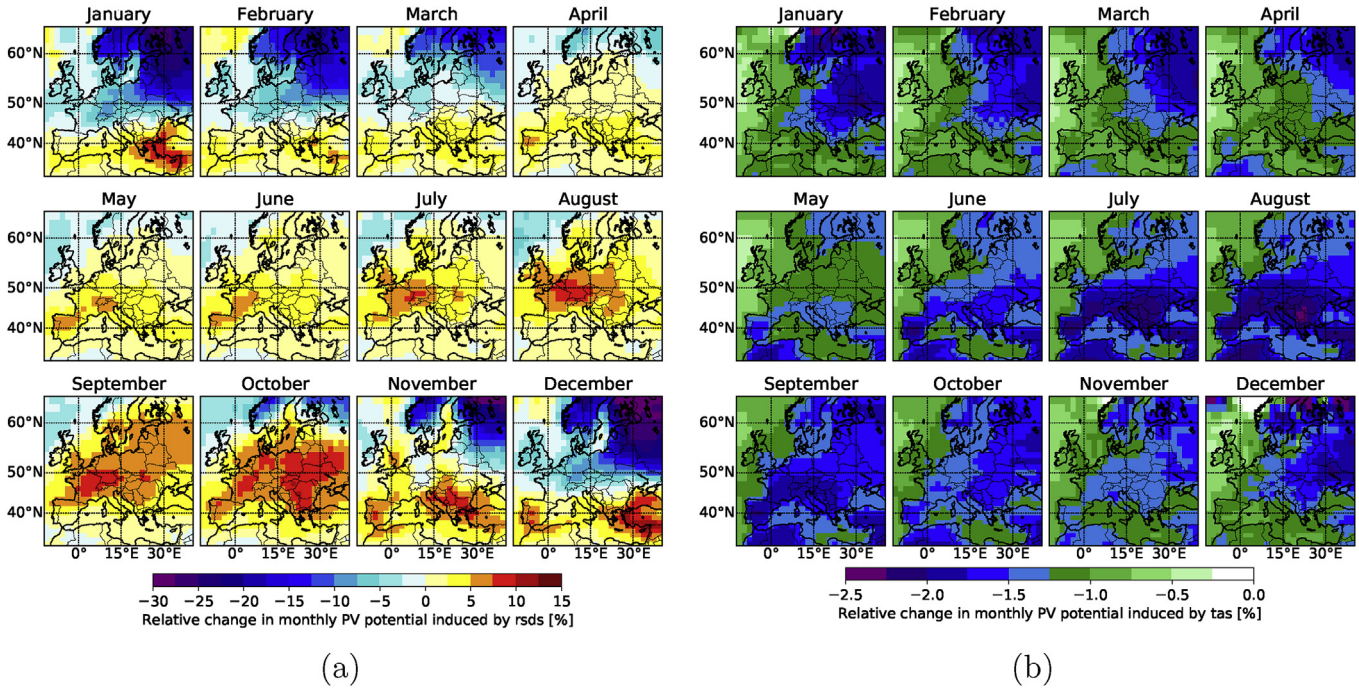

Fig. 11. Impact of *rsds* and *tas* on the monthly change in PV potential: The map shows the ensemble means of the change in monthly PV potential between the present (2007–2027) and future (2060–2080) time periods (RCP8.5) induced by changes in *rsds* (a) and *tas* (b), respectively.

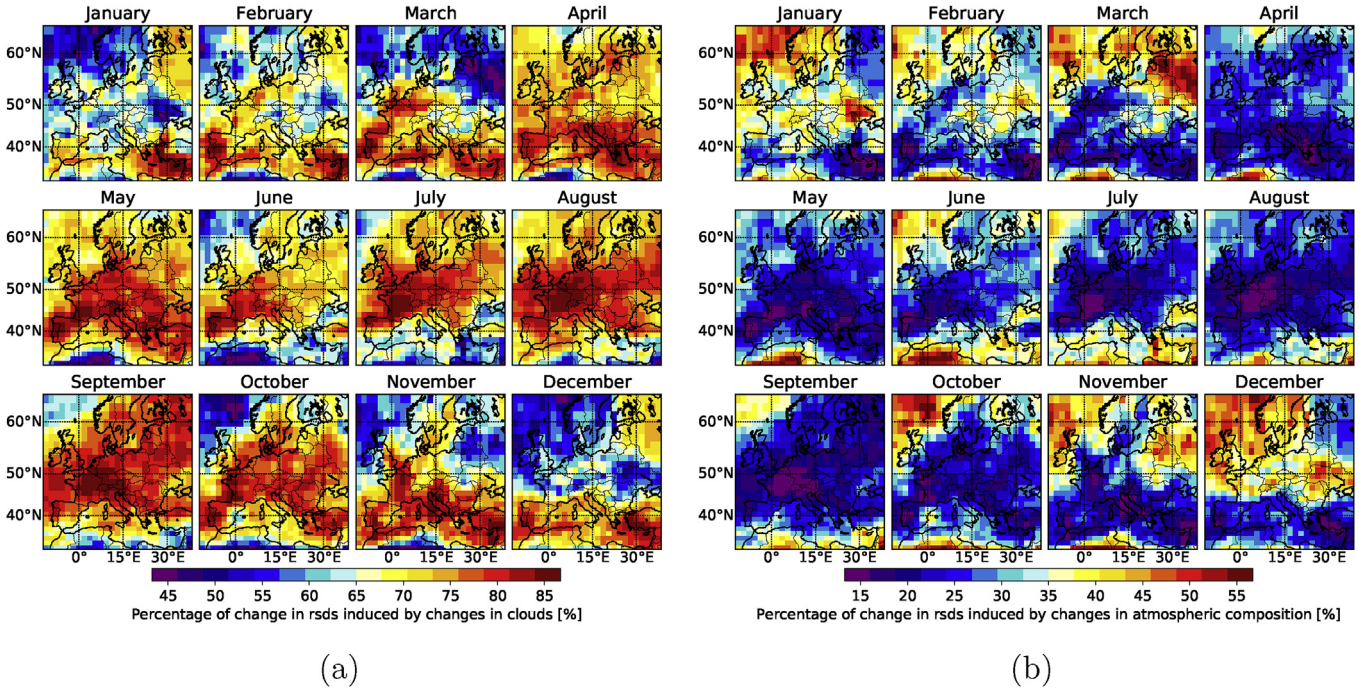

Fig. 12. Fraction of change in *rsds* caused by changes in clouds (a) and atmospheric composition (b) from the present (2007–2027) to the future (2060–2080) time period.

ranges from −30% to +10% and is statistically significant based on a two-sided *t*-test. Changes in winter, however, are not as severe since total PV yields in winter in the north are very low. The major share of PV potential change can be attributed to projected changes in irradiance, which in turn are caused for the most part by alterations in cloud characteristics. To put these results into perspective, we analyse how installed PV generation capacities expected by the European Commission's 2050 baseline scenario could be affected. We observe a positive impact for most European countries with only minor negative impacts in northern countries. This is due to the fact that the regions of increasing PV potential coincide with regions where the strongest growth in PV capacity is expected. This net effect over all European regions could translate into additional profits for PV system operators of 580 million per year through additional electricity sales. The negative economic impacts of climate change are of course projected to be orders of magnitude higher under an RCP8.5 scenario [6].

A comparison with other studies on this subject [7,24,35] shows mixed agreement (Tab. 4). Wild et al. [35] expect a positive trend in PV power output in Spain, France and south-eastern Europe on the order of 0.01–0.08%, which corresponds to a change of 0.5–4.3% in 2070. The pattern and magnitude of positive trend is similar to the results in this study, which can be expected, as both studies are based on CMIP5 data with RCP8.5. However, the negative change in northern and north-eastern Europe is not visible as a significant annual trend in Ref. [35]. This could be because they only evaluated trends up to 2049, rather than 2080 as in this study, and that the trend therefore did not yet have time to exit signal noise and enter significance.

Crook et al. [7] calculated the relative change of PV power in 2080 and received a similar pattern for positive change in PV potential, however with overall higher values for Spain, France, Germany central and south-eastern Europe. Crook et al. [7] also predicts a slight positive (0–4%) development in north-eastern Europe, contradicting our results (-4 - 0%). However, they only use a single model (HadGEM1 from CMIP3) with the SRES A1B emission scenario, which is one of the precursor scenarios of the RCPs. RCP8.5 and SRES A1B are of similar nature up to 2050, but then diverge. The emissions in SRES A1B decrease in the second half of the century, while for RCP8.5 they continue to increase and show a stronger similarity to SRES A1FI [21,33].

The results from Ref. [24] using the EURO-CORDEX RCMs differ from the results of this study. Jerez et al. [24] arrive at an almost uniform decrease of PV potential, except for some southern regions, where no significant change is projected. However, these large differences can be explained by the findings of [2]. That study compares projections for Surface Solar Radiation (SSR) in CMIP5 GCMs and EURO-CORDEX RCMs. The main factor responsible for the difference between the two appears to be different behaviour of cloud cover in global and regional climate models. In GCMs cloud cover shows a decrease throughout the next century, while RCMs project that it remains stable. RCMs even show a negative change in SSR in many places. This is explained with an increase of atmospheric absorption, which is also present in GCMs. However, in GCMs it does not manage to outweigh the effect of decreased cloud cover.

In our study we do not include future PV technology improvements, i.e. we assume that future PV technology has the same performance characteristics as today's. However, over the past decade the efficiencies of PV cell types and materials has increased on average by 0.17% per year (for crystalline silicon cells) [18]. This trend will likely continue in the future [22], so that energy yields from PV systems will be higher in 2060–2080 than today.

In light of our study, an increase in efficiency translates into higher absolute gains or losses potentially caused by climate change, while percentage losses would remain the same. Looking at regions with negative climate change impact, it is possible that higher cell efficiencies make up for some of the potential losses in absolute energy yield, when comparing a present with lower efficiencies to a future with higher efficiencies. In addition, it is also possible that future PV technologies have different performance characteristics with respect to their irradiance or temperature

response curves. Overall, however, we can expect a non-linear response of PV systems to irradiance to remain. Irrespective of PV technology, the question of how climatological factors and changes may impact PV power yield remains when planning concrete investments in this field.

Based on our study, we can expect overall potential PV yields in Europe to increase, although variability between countries is substantial. Countries where strong growth in the PV sector is expected, namely central and southern Europe, coincide with regions of increased PV yield caused by climate change. Hence investments in PV infrastructure in these regions will most likely produce more electricity in the future than today as some degree of climate change will affect Europe irrespective of mitigation actions taken now. Further investments in the PV sector in southern and central Europe should be seen as a no-regrets option, whereas in northern countries, under strong climate change, future PV installations may see some reduction in return on investment. However, we should note that the cost of PV are likely to fall further over the next decades as well [19]. Overall, our results suggest that investment into PV across Europe remains an attractive and no-regrets option irrespective of the degree of climate change in this century. If we consider that two key uncertainties not considered in our analysis, future PV cost and future PV efficiency, both most likely point towards improvements (higher efficiencies and lower costs, [19]), then this point is strengthened even further: in Europe, PV electricity generation is a no-regrets investment irrespective of climate change.

Appendix A. Supplementary data

Supplementary data to this article can be found online at https://doi.org/10.1016/j.energy.2018.12.139.

References

[1] Al-Sabounchi AM. Effect of ambient temperature on the demanded energy of solar cells at different inclinations. Renew Energy 1998;14(1–4):149–55.
[2] Bartok B, Wild M, Folini D, Lüthi D, Kotlarski S, Schär C, Vautard R, Jerez S, Imecs Z. Projected changes in surface solar radiation in CMIP5 global climate models and in EURO-CORDEX regional climate models for Europe. Clim Dynam 2016:1–19. 0123456789.
[3] Beiljing Climate Center. Climate System Models: BCC_CSM 1.1(m). 2018. http://forecast.bcccsm.ncc-cma.net/web/channel-63.htm.
[4] Burnett D, Barbour E, Harrison GP. The UK solar energy resource and the impact of climate change. Renew Energy 2014;71.
[5] Capros P, De Vita A, Tasios N, Siskos P, Kannavou M, Petropoulos A, Evangelopoulou S, Zampara M, Papadopoulos D, Nakos C. EU Reference Scenario 2016-Energy, transport and GHG emissions Trends to 2050. 2016.
[6] Ciscar J-C, Iglesias A, Feyen L, Szabó L, Van Regemorter D, Amelung B, Nicholls R, Watkiss P, Christensen OB, Dankers R, Garrote L, Goodess CM, Hunt A, Moreno A, Richards J, Soria A, feb. Physical and economic consequences of climate change in Europe. Proc Natl Acad Sci USA 2011;108(7):2678–83. http://www.ncbi.nlm.nih.gov/pubmed/21282624Ωhttp://www.pubmedcentral.nih.gov/articlerender.fcgi?artid=PMC3041092.
[7] Crook JA, Jones LA, Forster PM, Crook R. Climate change impacts on future photovoltaic and concentrated solar power energy output. Energy Environ Sci 2011;4(9):3101–9.
[8] Dervishi S, Mahdavi A, jun. Computing diffuse fraction of global horizontal solar radiation: A model comparison. Solar Energy 2012;86(6):1796–802 (Phoenix, Ariz.), http://www.ncbi.nlm.nih.gov/pubmed/27065498.
[9] Dunne JP, John JG, Adcroft AJ, Griffies SM, Hallberg RW, Shevliakova E, Stouffer RJ, Cooke W, Dunne KA, Harrison MJ. GFDL's ESM2 global coupled climate-carbon earth system models. Part I: Physical formulation and baseline simulation characteristics. J Clim 2012;25(19):6646–65.
[10] Elminir HK, Azzam YA, Younes FI. Prediction of hourly and daily diffuse fraction using neural network, as compared to linear regression models. Energy 2007;32(8):1513–23.
[11] ENES. European Earth System Models and Modelling groups. 2015. URL, https://portal.enes.org/models/earthsystem-models.
[12] ENES. CMIP5 Models and Grid Resolution. 2016. URL, https://portal.enes.org/data/enes-model-data/cmip5/resolution.
[13] EurObserv'ER. Photovoltaic Barometer 2010. 2010 [Tech. rep].
[14] EurObserv'ER. Photovoltaic Barometer 2017. 2017 [Tech. rep].
[15] European Energy Comission. EU - Energy modelling - interactive graphs. 2018. URL, https://ec.europa.eu/energy/en/content/energy-modelling-interactive-graphs.
[16] Folini D, Dallafior TN, Hakuba MZ, Wild M. Trends of surface solar radiation in unforced CMIP5 simulations. J Geophys Res 2017;122(1):469–84.
[17] Gaetani M, Huld T, Vignati E, Monforti-Ferrario F, Dosio A, Raes F. The near future availability of photovoltaic energy in Europe and Africa in climate-aerosol modeling experiments. Renew Sustain Energy Rev 2014;38:706–16.
[18] Green MA, Hishikawa Y, Dunlop ED, Levi DH, Hohl-Ebinger J, Ho-Baillie AWY. Solar cell efficiency tables (Version 1 - 52). Progress in Photovoltaics: Research and Applications. Jun ???? https://doi.org/10.1002/pip.3040.
[19] Haegel NM, Margolis R, Buonassisi T, Feldman D, Froitzheim A, Garabedian R, Green M, Glunz S, Henning H-M, Holder B, Kaizuka I, Kroposki B, Matsubara K, Niki S, Sakurai K, Schindler RA, Tumas W, Weber ER, Wilson G, Woodhouse M, Kurtz S. Terawatt-scale photovoltaics: Trajectories and challenges. Science apr 2017;356(6334):141–3. URL, http://science.sciencemag.org/content/356/6334/141.abstract.
[20] Huld T, Gottschalg R, Beyer HG, Topič M. Mapping the performance of PV modules, effects of module type and data averaging. Sol Energy 2010;84(2):324–38.
[21] IPCC. In: Nakicenovic Nebojsa, Swart Rob, editors. Special report on emissions scenarios (SRES), a special report of Working Group III of the intergovernmental panel on climate change. Cambridge University Press; 2000.
[22] ITRPV. International Technology Roadmap for Photovoltaic (ITRPV) 2018. 2018 [Tech. rep].
[23] Jacobson MZ, Jadhav V. World estimates of PV optimal tilt angles and ratios of sunlight incident upon tilted and tracked PV panels relative to horizontal panels. Sol Energy jul 2018;169:55–66. https://www.sciencedirect.com/science/article/pii/S0038092X1830375X{#}t0005.
[24] Jerez S, Tobin I, Vautard R, Montávez JP, López-Romero JM, Thais F, Bartok B, Christensen OB, Colette A, Déqué M, Nikulin G, Kotlarski S, van Meijgaard E, Teichmann C, Wild M. The impact of climate change on photovoltaic power generation in Europe. Nat Commun 2015;6:10014. http://www.nature.com/doifinder/10.1038/ncomms10014.
[25] Kawajiri K, Oozeki T, Genchi Y. Effect of temperature on PV potential in the world. Environ Sci Technol 2011;45(20):9030–5.
[26] Knutti R, Masson D, Gettelman A. Climate model genealogy: Generation CMIP5 and how we got there. Geophys Res Lett 2013;40(6):1194–9.
[27] Kost C, Mayer JN, Thomsen J, Hartmann N, Senkpiel C, Philipps S, Nold S, Lude S, Saad N, Schlegel T. Levelized Cost of Electricity Renewable Energy Technologies. Fraunhofer Institut for Solar Energy Systems Ise Levelized; 2013. p. 2–5 (November).
[28] Panagea IS, Tsanis IK, Koutroulis AG, Grillakis MG. Climate change impact on photovoltaic energy output: the case of Greece. Adv Meteorol 2014;2014.
[29] Pfenninger S, Staffell I. Long-term patterns of European PV output using 30 years of validated hourly reanalysis and satellite data. Energy 2016;114:1251–65.
[30] Ridley B, Boland J, Lauret P. Modelling of diffuse solar fraction with multiple predictors. Renew Energy 2010;35(2):478–83. https://doi.org/10.1016/j.renene.2009.07.018.
[31] Stocker TF, Qin D, Plattner G-K, Tignor M, Allen SK, Boschung J, Nauels A, Xia Y, Bex V, Midgley PM. Summary for policymakers. In: Climate Change 2013: The Physical Science Basis. Contribution of Working Group I to the Fifth Assessment Report of the Intergovernmental Panel on Climate Change. CEUR Workshop Proceedings, vol. 1542; 2015. p. 33–6.
[32] Torres JL, De Blas M, García A, de Francisco A. Comparative study of various models in estimating hourly diffuse solar irradiance. Renew Energy 2010;35(6):1325–32.
[33] van Vuuren DP, Edmonds J, Kainuma M, Riahi K, Thomson A, Hibbard K, Hurtt GC, Kram T, Krey V, Lamarque JF, Masui T, Meinshausen M, Nakicenovic N, Smith SJ, Rose SK. The representative concentration pathways: An overview. Climatic Change 2011;109(1):5–31.
[34] Watanabe S, Hajima T, Sudo K, Nagashima T, Takemura T, Okajima H, Nozawa T, Kawase H, Abe M, Yokohata T. MIROC-ESM 2010: Model description and basic results of CMIP5-20c3m experiments. Geosci Model Dev (GMD) 2011;4(4):845.
[35] Wild M, Folini D, Henschel F, Fischer N, Müller B. Projections of long-term changes in solar radiation based on CMIP5 climate models and their influence on energy yields of photovoltaic systems. Sol Energy 2015;116:12–24.
[36] Wirth H, Schneider K. Recent facts about photovoltaics in Germany. Germany: Report from Fraunhofer Institute for Solar Energy Systems; 2015. p. 26.
[37] Yadav AK, Chandel S, jul. Tilt angle optimization to maximize incident solar radiation: A review. Renew Sustain Energy Rev 2013;23:503–13. https://www.sciencedirect.com/science/article/pii/S1364032113001299.